EVALUATING THE HYDRATION OF HIGH VOLUME FLY ASH MIXTURES USING CHEMICALLY INERT FILLERS

Igor De la Varga[a], Javier Castro[b], Dale Bentz[c], Franco Zunino[b,d], and W. Jason Weiss[e]

[a] Federal institute of highway administration (FHWA)
[b] Faculty of Engineering, Universidad del Desarrollo, Av. La Plaza 680 Las Condes, Santiago, Chile.
[c] National institute of Standards and Technology (NIST)
[d] Laboratory of Construction Materials, EPFL STI IMX LMC Station 12, CH-1015 Lausanne, Switzerland. franco.zunino@epfl.ch

ABSTRACT: Fly ash is frequently used as a replacement for cement in concrete. However, questions remain regarding the influence that fly ash has on the hydration of cement. This paper examines physical aspects (e.g., surface nucleation, cement particles spacing) and chemical aspects (e.g., pozzolanic and hydraulic reactions) of the fly ash and cement in mixtures containing high volumes of fly ash. In addition to using fly ash, a chemically inert filler was used consisting of a blend of fine silica sands with approximately the same particle size distribution as that of the fly ash. The paper compares reactivity results from 1) cement, 2) cement-fly ash and 3) cement-inert filler systems. Isothermal calorimetry, internal relative humidity and electrical conductivity measurements are used to better evaluate the role played by the fly ash in these systems at later ages. The internal relative humidity assesses self-desiccation in a sealed system, which is an indication of the ongoing chemical reaction, while the electrical measurements assess transport properties and the type of microstructure that forms. These parameters can be used to evaluate the extent of reaction at later ages. The results provide a decoupling of the physical and chemical effects of high volume fly ash on cement hydration at early and later ages.

Keywords: Filler effect; high volume fly ash; hydration; internal relative humidity; isothermal calorimetry.

1. INTRODUCTION

Fly ash is a by-product of coal combustion that has been broadly used by the concrete industry as a supplementary cementitious material (SCM) [1–9]. Fly ash can be used to replace cement, which decreases the clinker factor and embodied CO_2 [10–12] and generally improves workability and durability [13]. High Volume Fly Ash (HVFA) mixtures are typically designed with more than 50 % (by mass) of the cement replaced with fly ash. Fly ash is less reactive than cement. Fly ash can sometimes cause retardation and extended setting times, especially when employed at higher volumes [14–16]. The degree of reactivity for the fly ash depends on the type of fly ash used (e.g., a Class C fly ash has typically more hydraulic properties than a Class F fly ash, being more reactive in the presence of moisture) [17]. With both classes of fly ash, lower strengths are typically observed in HVFA concrete at early ages [18]. Typically, it is possible to counteract this strength loss by reducing the water-to-cementitious ratio [19], using accelerating additions, replacing a portion of the fly ash with a fine limestone powder, or switching to a more reactive Type III cement [20–24].

The reactivity of fly ash and its effect on cement hydration has been a focus of study throughout the 20th and into the 21st century [19-23]. It now becomes more relevant to understand due to the current tendency of using larger amounts of fly ash to replace cement in concrete.

The reaction kinetics of fly ash-cement systems is complicated by the fact that the reactions of the cement and fly ash may interact and, more importantly, by the difficulty in measuring the degree of reaction of these two components independently [25]. Recently, several studies had focused on developing faster and more reliable techniques for physical and chemical characterization of fly ash that can be related to fly ash reactivity [26–32].

It is generally accepted that concrete containing fly ash is more durable than conventional ordinary portland cement (OPC) concrete, due mainly to the pore refinement produced by the pozzolanic reaction that converts the calcium hydroxide ($Ca(OH)_2$) formed during cement hydration to additional calcium silicate hydrate gel (C-S-H), resulting in a reduction in the permeability/diffusivity of the matrix [33,34]. The pozzolanic reaction can also cause a size reduction and densification of the interfacial transition zone (ITZ) region between the aggregates and the cement matrix, often considered to be a weak interface due to the higher porosity as compared to the bulk matrix. The reaction between fly ash and the ($Ca(OH)_2$) in this ITZ region reduces its local porosity.

According to ASTM C595, a pozzolan is defined as ‘‘a siliceous or siliceous and aluminous material, which in itself possesses little or no cementitious value but will, in finely divided form and in the presence of moisture, chemically react with calcium hydroxide to form compounds possessing cementitious properties (pozzolanic activity).’’ Fly ash is one of the materials that falls into this category. The pozzolanic reaction typically starts at later ages, since fly ash needs $Ca(OH)_2$ formed during cement hydration for the reaction. Depending on the fly ash characteristics and the alkalinity of the pore solution, its reaction with $Ca(OH)_2$ will occur earlier or later [33,35]. It is often thought that the pozzolanic effect is more dominant than any other effects (e.g., filler effects) [36–38], especially at later ages.

A common technique to determine the reactivity of cementitious materials is by using an isothermal calorimeter. The hydration reaction is exothermic; therefore, measuring the heat release of these materials indicates how much of the material has reacted. When comparing the heat release between plain cement and fly ash-cement systems, it can be mistakenly interpreted that the difference in heat release between these two systems is solely due to the fly ash reactivity. Typical cumulative heat release curves for cement and cement-fly ash pastes are shown in Figure 1 where the heat release per g of cement of a 100 % OPC and a 40 % (by volume) fly ash – 60 % OPC systems are plotted as a function of time. In the conventional practice of normalizing the heat release per g of cement (as in Figure 1), the fly ash is considered to act as an inert material; therefore, the difference in heat observed is purely due to the presence of fly ash, which can have physical and/or chemical effects on the cement hydration, instead of just providing additional chemical reactions (hydraulic and pozzolanic) that increases the heat release. Inert fillers with similar particle size distributions (PSD) to the pozzolanic materials under study have been used in an attempt to decouple the chemical and physical effects of SCMs using compressive strength measurements [39].

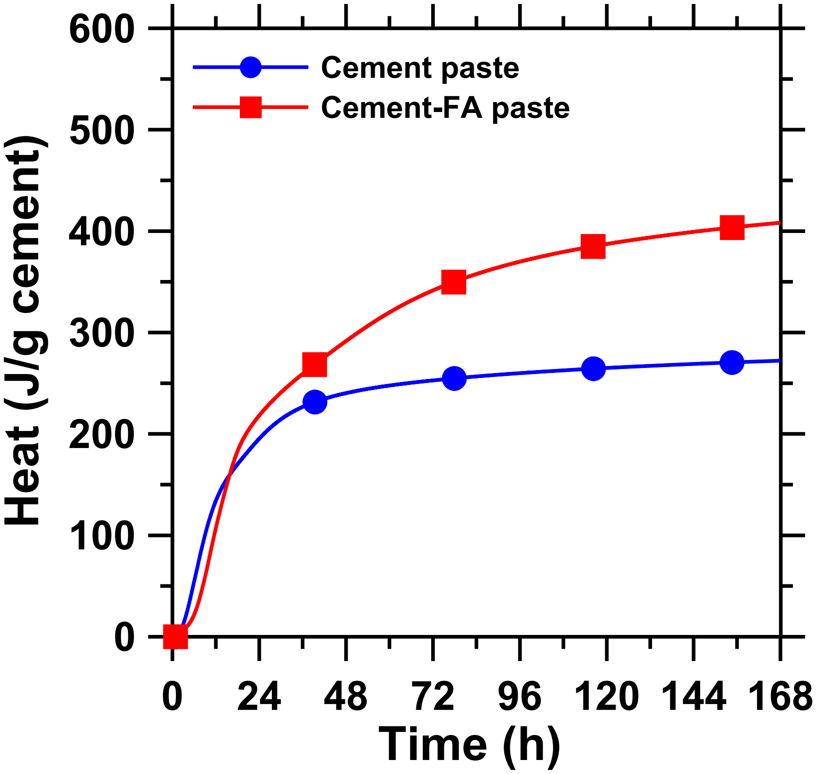

Figure 1. Examples of measured heat release in cement and cement-fly ash blended pastes. Uncertainty for these values will be presented later in the text (Figure 5 discussion).

The present investigation explores the idea that the chemical reactivity of the fly ash is not the only aspect to consider when fly ash is mixed with cement. Fly ash can also act as a filler [19], especially at very early ages, prior to its reaction. In addition, retardation of the initial hydration reactions of cement (and consequently, of initial setting time) due to dilution and interaction with some fly ash components are commonly observed [21,40], as it would happen in systems containing other fillers [41–43]

As mentioned above, the reactivity of the fly ash, particularly Class F fly ash, depends on the alkalinity of the pore solution and the availability of $Ca(OH)_2$, both of which build up over a few days. Therefore, the amount of reaction of fly ash in the first day or so is often negligible and changes in hydration kinetics may be dominated by the physical filler effect. Two combined physical effects may occur; 1) dilution (i.e., larger separation distances among cement particles), which promotes a better cement hydration since more surfaces are exposed, and 2) provision of new nucleation sites via the fly ash surfaces that will promote the formation of additional hydration products. A graphical representation of these two concepts is shown in Figure 2. This was done by adapting a hard core-soft shell (HCSS) model developed at NIST [40,44]. In this case, the model was used to represent a system where cement particles (red color) of different sizes (according to the particle size distribution of the cement used in this study) are randomly distributed in a three-dimensional volume. The same particle size distribution was used where 60 % (by volume) of the cement particles were replaced with either fly ash or inert filler (blue color). The image on the left represents a water-to-cement ratio, *w/c* = 0.30 plain system with just cement particles, whereas the image in the center corresponds to the same *w/c* = 0.30 system, but with 60 % of the cement particles (by volume) being replaced with fly ash (or inert filler), thereby increasing the number of potential nucleation sites. Finally, the image on the right shows a system where the fly ash (or inert filler) particles are removed, thus increasing the cement particles' spacing (which would correspond to a *w/c* = 0.67 plain system).

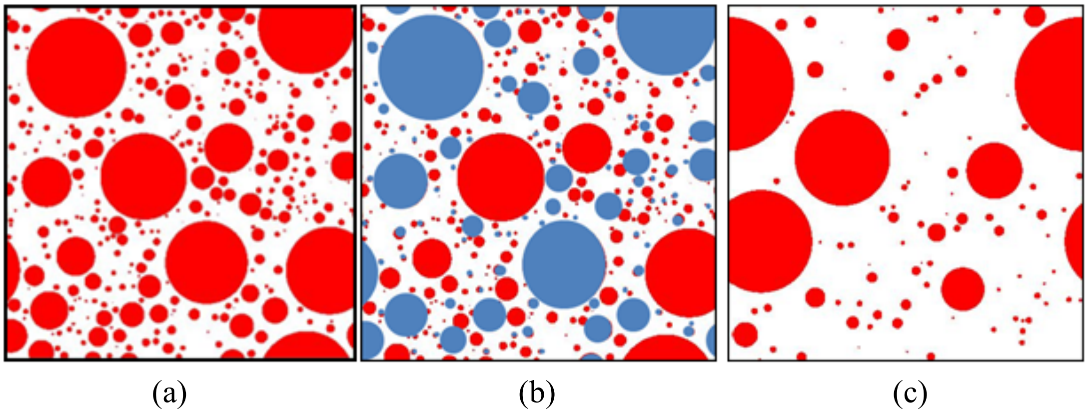
(a) (b) (c)

Figure 2. (a) *w/c* = 0.30 plain system, (b) *w/c* = 0.30-60 % fly ash (or inert filler) system, and (c) *w/c* = 0.67 plain system

2. OBJECTIVE

The objective of this study is to better understand the chemical contribution of fly ash as a reactive element (i.e., its pozzolanic or chemical activity) and its physical contributions as a nucleation agent and increasing the cement particle spacing. Three different aspects will be analyzed:

1) Evaluate the physical and chemical effect that high levels of fly ash replacement have on the cement hydration. This would include the aspects of pozzolanic reaction, additional nucleation sites, and increased cement particle spacing.

2) Isolate the physical effect (nucleation and cement particle spacing) from the chemical effect (pozzolanic reaction).

3) Differentiate, within the physical effect, between the contribution of fly ash on the provision of nucleation sites and increased cement particle spacing.

3. MATERIALS

An ASTM C150-09 Type I/II OPC was used in this study, with a Blaine fineness of 476 m^2/kg, a density of 3170 kg/m^3 ± 10 kg/m^3, an estimated Bogue potential phase composition of 52 % C_3S, 18 % C_2S, 8 % C_3A, and 9 % C_4AF by mass, and a Na_2O equivalent of 0.5 % by mass. A Class C fly ash (ASTM C618-08a) was also used with a density of 2630 kg/m^3 ± 10 kg/m^3. Silica sand with an apparent specific gravity of 2.65 was used as the fine aggregate. The chemically inert (hereafter designated as inert) filler used to replace the fly ash consisted of a combination of two size fractions of fine silica sand (SIL-5 and SIL-40) with a very similar density to that of the fly ash used, 2650 kg/m^3 ± 10 kg/m^3. (Here it is assumed that even the smallest particles of this material are chemically inert). Table 1 shows the chemical compositions of the materials used in the study.

Table 1. Chemical composition (wt. %) of the cement, fly ash, fine aggregate, and inert filler. (Uncertainty was determined to be ± 0.1 for values ≥ 0.1 %, and ± 0.01 for values < 0.1 %)

	Cement	Fly Ash	Fine Aggregate	SIL-5	SIL-40
SiO_2, %	20.0	38.7	99.7	98.5	99.5
Al_2O_3, %	4.8	19.2	0.1	1.00	0.3
Fe_2O_3, %	2.9	6.5	0.02	0.1	0.02
CaO, %	63.3	23.5	< 0.01	0.04	0.02
MgO, %	1.5	5.3	< 0.01	0.02	0.01
SO_3, %	3.3	1.4	-	-	-
K_2O, %	0.4	0.6	< 0.01	0.04	0.01
Na_2O, %	0.3	1.6	< 0.01	0.02	0.01
Loss on Ignition, %	2.9	0.3	0.1	0.4	0.1

Figure 3 shows the particle size distribution (PSD) of the fly ash used in the study. Two gradations of fine silica sand were chosen to comprise the inert filler. The two gradations selected (SIL-5 and SIL-40) were combined to have a similar PSD to that of the fly ash as shown in Figure 3. The mass proportions used in the combination were 16.67 % and 83.33 % of the SIL-5 and SIL-40, respectively. The result shown for fly ash is the average of six individual measurements and the error bars (one standard deviation) would fall within the size of the shown symbols.

It is important to note at this point that although the PSD obtained when combining two fractions of inert filler is similar, it is not identical to that of the fly ash. Also the angular shape of the inert filler (due to grinding) will be different from the generally round shape of the fly ash particles, potentially providing a different amount of nucleation sites (surfaces). As a reference point, for ground cement particles, their surface area is increased by about a factor of 1.4 relative to spherical particles of an equivalent volume [45].

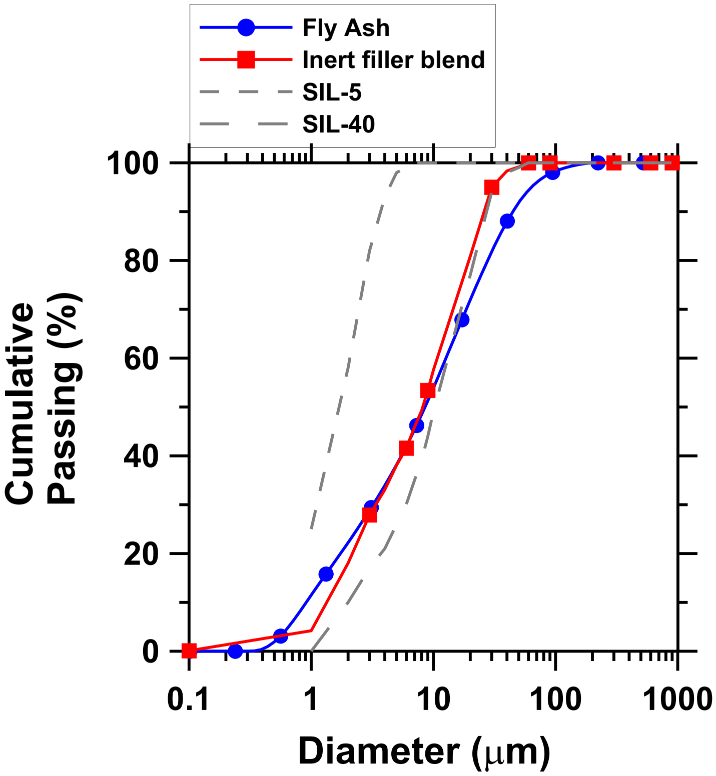

Figure 3. Cumulative PSD of the fly ash, inert filler blend, and the two inert filler fractions combined to form the inert filler blend.

4. MIXTURE PROPORTIONS

A total of nine mortar mixtures with 55 % of fine aggregate volume fraction were prepared. All mortars were prepared in a Hobart blender according to the mortar mixing procedure described in ASTM C305 [46]. The mixture proportions are shown in Table 2. The term *w/c* is used when the cementing phase is just cement, whereas *w/cm* is used when either fly ash or inert silica sand are used in the cementing fraction. The reasons for choosing each of the mixture proportions are presented below:

- Mixtures prepared to accomplish objective #1. Four mortars were prepared with *w/c* = 0.30 and w/*cm* = 0.30: a plain mortar (M1), and three mortars containing different fly ash volume replacements (M2, M3, M4), with the fly ash replacing the volume of cement in M1 at volume replacement levels of 40 %, 60 %, and 80 %, respectively.
- Mixtures to accomplish objective #2: Three mortars (M5, M6, and M7) were prepared with *w/cm* = 0.30. In these mortars an inert filler (IF) is used to replace the cement in the same proportions as in M2, M3, and M4. The use of the inert filler corresponds to an equivalent system to that obtained in the fly ash mortars, without providing a chemical effect, thus isolating the physical action (i.e., M2 is similar to M5).
- Mixtures to accomplish objective #3: Two mortars were prepared with *w/c* of 0.47 and 0.67 (with neither inert filler nor fly ash). These *w/c* correspond to the same *w/c* used in mortars M2 and M3 (and therefore, M5 and M6), respectively. These systems would correspond to a similar cement particle spacing distribution in the matrix, without providing additional nucleation sites, in other words, just considering the cement particles' spacing. These mortars are labeled as M8 and M9. (NOTE: An attempt to reproduce the cement particles' spacing of the mortar containing 80 % of either fly ash or inert filler was performed. This mortar mixture would have had a *w/c* = 1.30, but showed severe segregation/bleeding issues. Therefore, it was decided by the authors to not include this mixture in the analysis).

Table 2. Mortar mixture proportions used in the study

	M1	M2	M3	M4	M5	M6	M7	M8	M9
w/c	0.30	0.47	0.67	1.30	0.47	0.67	1.30	0.47	0.67
w/cm	0.30	0.30	0.30	0.30	0.30	0.30	0.30	0.47	0.67
Fly Ash, vol. %	-	40	60	80	-	-	-	-	-
Inert Filler, vol. %	-	-	-	-	40	60	80	-	-
Cement, kg/m^3	731	453	307	156	453	307	156	573	456
Water, kg/m^3	210	207	206	203	207	203	199	269	306
Fly Ash, kg/m^3	0	252	384	521	0	0	0	0	0
Inert Filler, kg/m^3	0	0	0	0	252	384	521	0	0
Fine Aggregate, kg/m^3	1457	1457	1457	1457	1457	1457	1457	1457	1457

5. EXPERIMENTAL PROCEDURES

5.1. Isothermal Calorimetry

Measurement of the heat release due to the exothermic reaction of cementitious materials can be used to assess the reaction of a cementitious system. The difference in heat release can be used to quantify the influence of fly ash or inert fillers. Approximately 5 g of the externally mixed mortar mixtures shown in Table 2 were weighed and placed in a glass ampoule, which was then capped and placed into the calorimeter about 10 min after cement was first mixed with water and then monitored for up to 7 d. The heat release and rate of heat release were determined. Previously, the average absolute difference between replicate specimens was measured to be 2.4 x 10^{-5} W/g (cement) with a maximum absolute difference of 0.00011 W/g (cement), for measurements conducted between 1 h and 7 d after mixing [47].

5.2. Internal Relative Humidity

As cement hydrates, water is consumed. Chemical shrinkage occurs when cement reacts with water as the reacted products occupy a smaller volume than the initial constituents [48,49]. Chemical shrinkage, after the time of set, results in the creation of vapor-filled spaces within the matrix [50]. This is commonly referred to as self-desiccation, directly causing a decrease in the measured internal Relative Humidity (RH). Thereby, direct RH measurements can also be helpful for assessing reactivity. In this study, RH measurements were performed during 7 d of reaction on mortar samples that were crushed approximately 8 h after cement-water contact. Using Rotronic HygrClip2S humidity sensors[1] (± 0.8 % RH at 23 °C ± 0.1 °C) the data were recorded at 5 min intervals. The probes were mounted in a 75 mm x 68 mm stainless steel cylinder that was placed over a water jacketed sample cup holder. The water jacket was connected to a programmable water bath maintained at a constant temperature of 23 °C ± 0.1 ºC. The 10 g samples were placed in 12 mm deep cups with a 43 mm diameter. The sensors were also employed to measure the RH above slurries of reference salts (potassium sulfate, potassium chloride, and sodium chloride) to provide points of calibration [51].

Additional samples were kept sealed in plastic containers and double bags for different periods of time: 28 d and 1 year. These samples were crushed and inserted in the cup holders to measure the internal RH at those ages.

5.3. Electrical Conductivity

In cement-based materials, it is commonly accepted that the fluid phase is very conductive compared to that of the solid or vapor phases. If the electrical conductivity of the porous system is measured, this can be used to infer the extent of the hydration reaction and characteristics of the pore structure such as pore volume and connectivity.

---

[1] Certain commercial products are identified in this paper to specify the materials used and procedures employed. In no case does such identification imply endorsement or recommendation by SES Group and Associates, the National Institute of Standards and Technology, Oregon State University, or Universidad del Desarrollo, nor does it indicate that the products are necessarily the best available for the purpose.

Three samples of each mortar were prepared in cylindrical molds of 70 mm height and 35 mm diameter. Two 2.5 mm rods, spaced 20 mm apart, were embedded longitudinally inside each sample to act as electrodes. The experimental set-up is shown in Figure 4. The electrical resistance was directly measured using a Solatron 1260 Impedance Gain-Phase analyzer with a frequency range of 1 MHz to 10 Hz, and a 500 mV AC Signal. The measured electrical resistance (taken as the real component achieved at the frequency when the imaginary component crossed or approached its zero axis), must be corrected by a geometry factor to determine the electrical resistivity using equation 1.

$$\sigma = \frac{1}{R \cdot k} \tag{1}$$

where σ is the mortar electrical conductivity ($1/\Omega \cdot \text{m}$), R is the measured mortar electrical resistance (Ω), and k is the geometry factor, determined to be 0.044 m for this study [52].

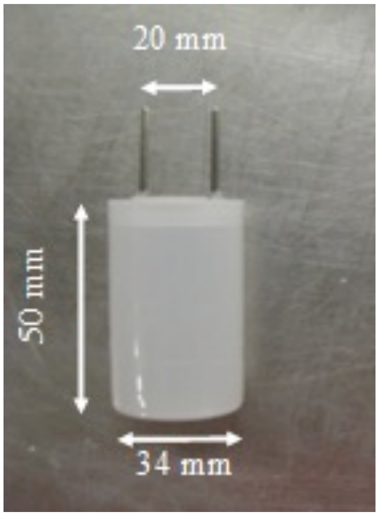

Figure 4 Sample mold for electrical conductivity measurements.

The electrical conductivity measurements were performed at 3 months and 6 months on the sealed mortar specimens.

6. EXPERIMENTAL RESULTS AND DISCUSSION

6.1. Isothermal Calorimetry

Figures 5 and 6 show the measured heat release and heat flow per gram of cement for the control mixture (*w/c* = 0.30 plain) and the mixtures containing 40 % by volume of either fly ash or inert filler. The plain mixture with *w/c* = 0.47 is also included since it represents the same cement particle spacing as those having a volume replacement level of 40 %. As mentioned before, normalizing the heat release per gram of cement would result in all the plots being similar if the fly ash is inert. One aspect to point out is that the low *w/c* mixture (M1) could undergo significant self-desiccation at later ages, which might bias the comparison with the other three mixtures that are expected to exhibit a lower amount of self-desiccation. As such, a layer of water was added on top of the M1 specimen to minimize self-desiccation. Figure 5 shows differences in the heat release among the four mixtures. The magnitudes of these differences are indicated with arrows in the figure and preliminarily attributed to different effects (physical and/or chemical). For reference, the single operator uncertainty for 7 d cumulative heat release provided in ASTM C1702 [53] is 3.6 % that would correspond to about 10 J/g cement at 7 d for the data in Figure 5.

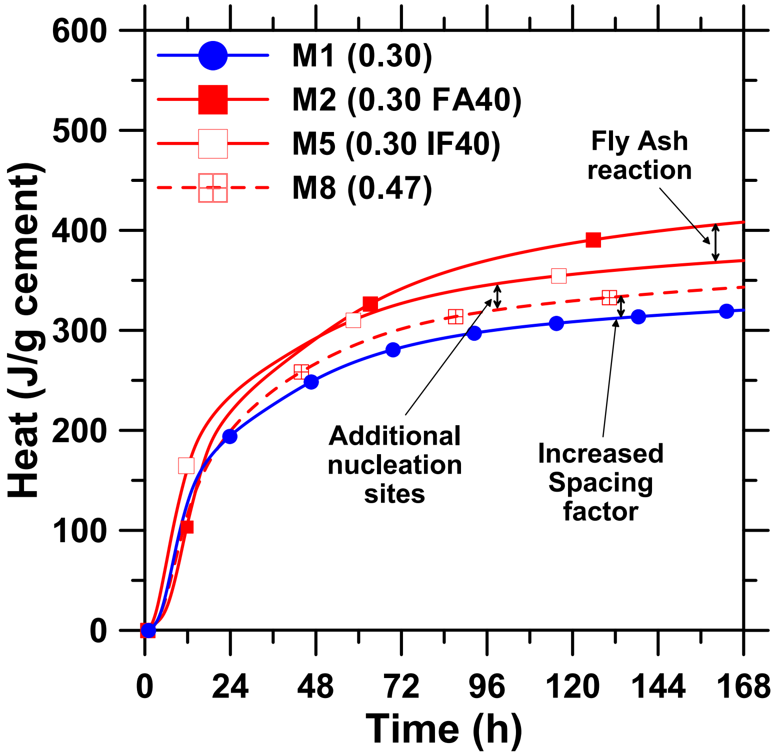

Figure 5. Heat release as a function of time. Comparison between *w/c* = 0.30 plain, *w/cm* = 0.30 + 40 % fly ash or inert filler, and *w/c* = 0.47 plain mortar mixtures.

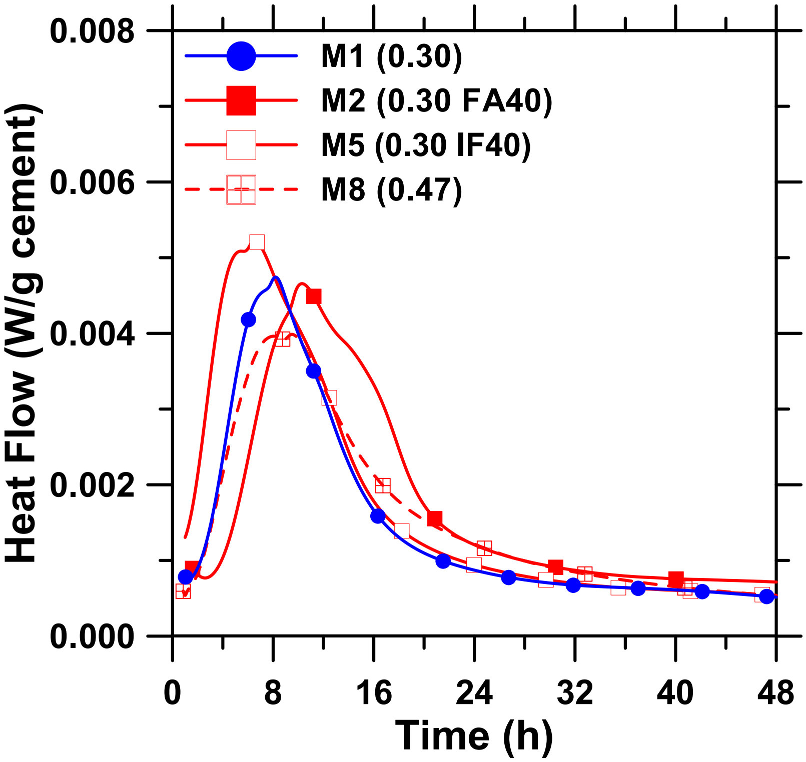

Figure 6. Heat flow as a function of time. Comparison between *w/c* = 0.30 plain, *w/cm* = 0.30 + 40 % fly ash or inert filler, and *w/c* = 0.47 plain mortar mixtures.

In Figure 7, the total amount of heat release by the fly ash mixture has been separated into the three effects indicated in Figure 5: increased spacing, nucleation and fly ash reaction. These would have to be added to the heat released by the *w/c* = 0.30 mixture (M1) to add up to the total represented by the fly ash mixture (M2). This was done by subtracting the amount of heat release among the curves. For instance, the heat attributed to spacing was calculated by subtracting the heat of M1 from the heat of M8. In Figure 7, the curves of each effect are presented in a stacked area array to visualize the gap filling between the M1 and M2 curves.

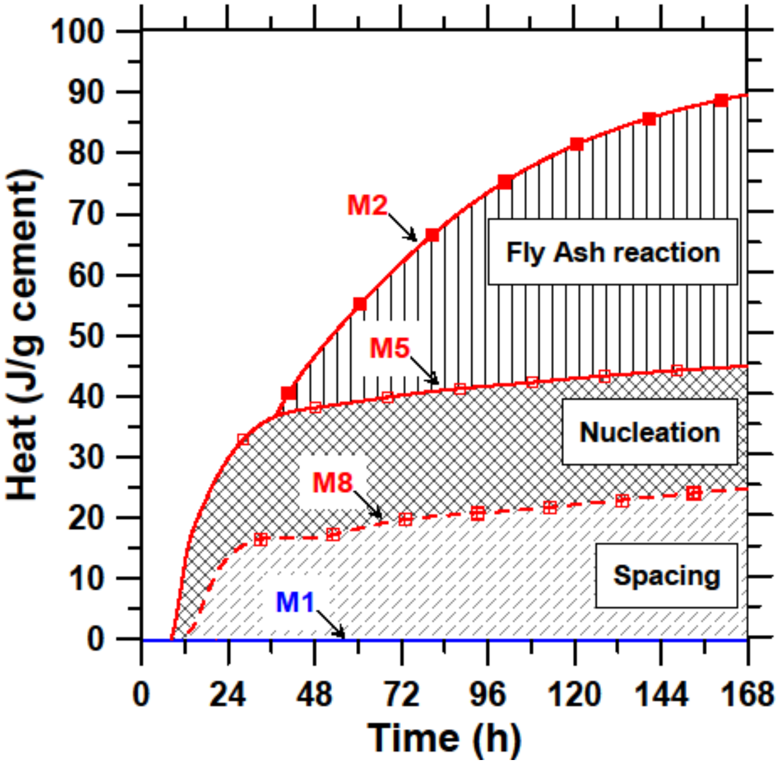

Figure 7. Additional heat (in reference to M1) attributed to increased spacing factor, additional nucleation sites, and fly ash reaction in a *w/cm* = 0.30 mortar with 40 % of the cement volume being replaced.

When comparing specimens M1 and M8 from Figure 5, a higher heat release is achieved in M8, being 8 % larger at 7 d. This is attributed to the increased cement particle spacing that promotes a further hydration. While there is practically no difference in the cumulative heat release during the first 24 h between M1 and M8 (as should be expected since the samples maintain high humidity at very early ages), the results in Figure 6 show that the lower *w/c* mixture (M1) presents greater heat flow compared to M8. The same effect was also observed by Castro et al. [54]. This might be attributed to the mixing intensity. Bentz et al. [55] observed nearly identical heat release curves for cement pastes of different *w/c* prepared in a high shear blender; however, they found a greater dispersion between curves for mortars of different *w/c* prepared in a Hobart mixer based on ASTM C305 [46], with the lower *w/c* mortars showing earlier heat release and accelerated setting. According to this, the more viscous mortar receives more energy input during the mixing phase which might produce a better dispersion of the cement particles and a greater rate of initial hydration as observed in Figure 6. The magnitude of this effect is negligible at later ages. In addition, a more concentrated pore solution in the lower *w/c* system (M1) compared to M8 may also increase the initial rate of hydration of the mixture.

The mixture with inert filler (M5) has 14 % more heat release at 7 d than that of M1. This percentage is the combination of the above mentioned 8 % (increased cement particle spacing) and an additional 6 % corresponding to the increased number of available nucleation sites (assuming that fly ash and the inert filler have the same surface area and the same ability for providing nucleation sites). A faster rate of heat release and larger heat flow peak in M5 compared to M1 can also be observed in Figure 6, directly attributed to the provision of additional nucleation sites.

When comparing M1 and M2 in Figure 5, the difference in heat release is 28 % at 7 d. This would correspond to increases of 14 % due to fly ash reaction, 6 % due to the increased number of nucleation sites, and 8 % due to the increased cement particle spacing. In addition to this, a 4-h retardation period is observed in M2 (Figure 6). It seems that this retardation effect is larger than the possible filler effect provided by the fly ash (as the first peak or main silicates reaction happens later than in M1). In this case, the fly ash probably reacts with some of the calcium ions, diluting their concentration in the pore solution and thus lengthening the induction period [35], although retardation of early-age hydration by fly ash can also be due to other reasons, including sulfate imbalance. At the time that the required calcium concentration is achieved, the main silicates reaction takes place. Despite the fact that M5 and M2 have the same cement volume replacement level, M5 has a higher surface area than M2 (due to grinding of the inert filler). The higher surface area might provide a higher nucleation effect, accelerating the reaction. Also, the inert filler used in M5 has no absorption of water compared to the fly ash in M2 which might have a little absorption. This effect would leave more available water (-filled space) in the M5 system than in M2, so that its cement particles might react faster.

In Figure 7, it can be observed that just the nucleation and spacing effects are detected during the first 36 h of hydration, the former starting to be measurable slightly earlier than the latter. This can be explained as additional nucleation sites can provide templates for C-S-H precipitation before the increased spacing and water availability makes a measurable difference compared to M8. However, this temporal shift between both components of the physical effect of fly ash will depend on the particular characteristics of the system studied, such as *w/c* and replacement level. At 36 h of hydration, the fly ash reactions start having a measurable effect as well. At 7 d, it can be observed that the physical (spacing and nucleation) and chemical contributions of fly ash account for around 50 % each of the additional heat release of M2 compared to M1.

The same type of analysis can be done in the other two systems (60 % and 80 % volume replacement levels). Figures 8-11 show the results for these two systems. It can be noticed that the same trends as those in the 40 % system are observed in terms of increased heat release and acceleration/retardation effects, although with higher heat flow peaks and larger separation among heat curves as the volume replacement level increases. This is due to the type of normalization used (per g of cement).

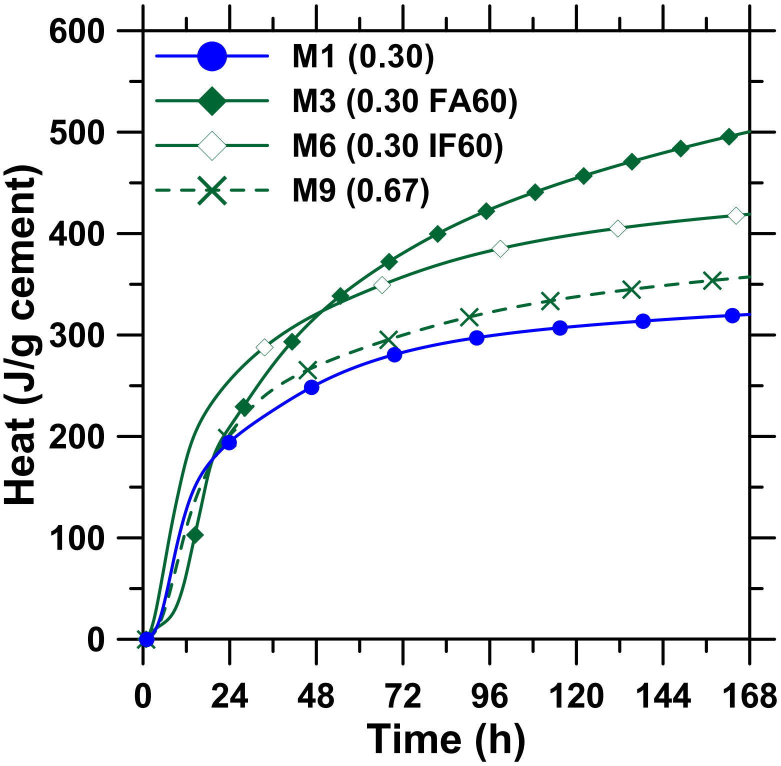

Figure 8. Heat release as a function of time. Comparison between *w/c* = 0.30 plain, *w/cm* = 0.30 + 60 % fly ash or inert filler, and *w/c* = 0.67 plain mortar mixtures.

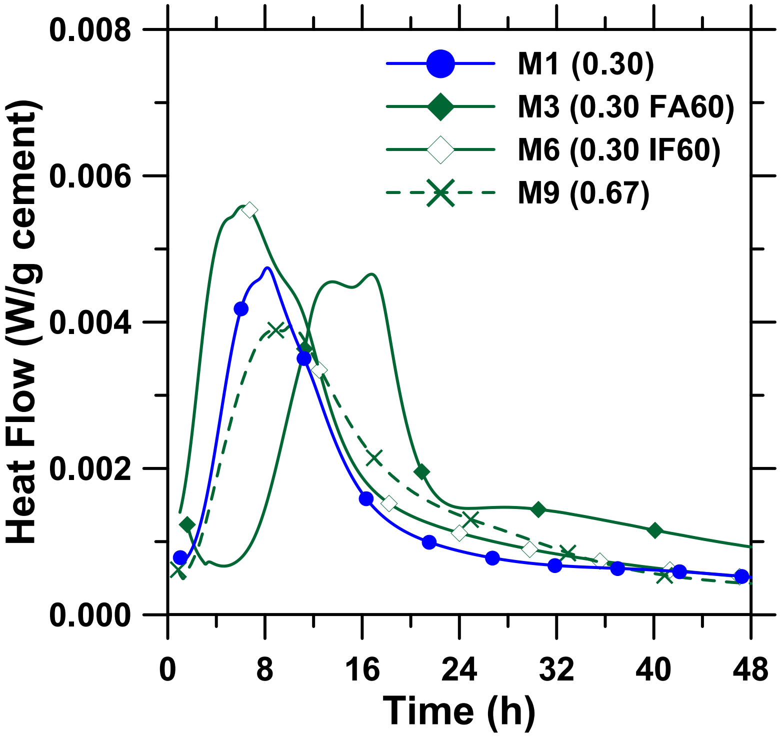

Figure 9. Heat flow as a function of time. Comparison between *w/c* = 0.30 plain, *w/cm* = 0.30 + 60 % fly ash or inert filler, and *w/c* = 0.67 plain mortar mixtures.

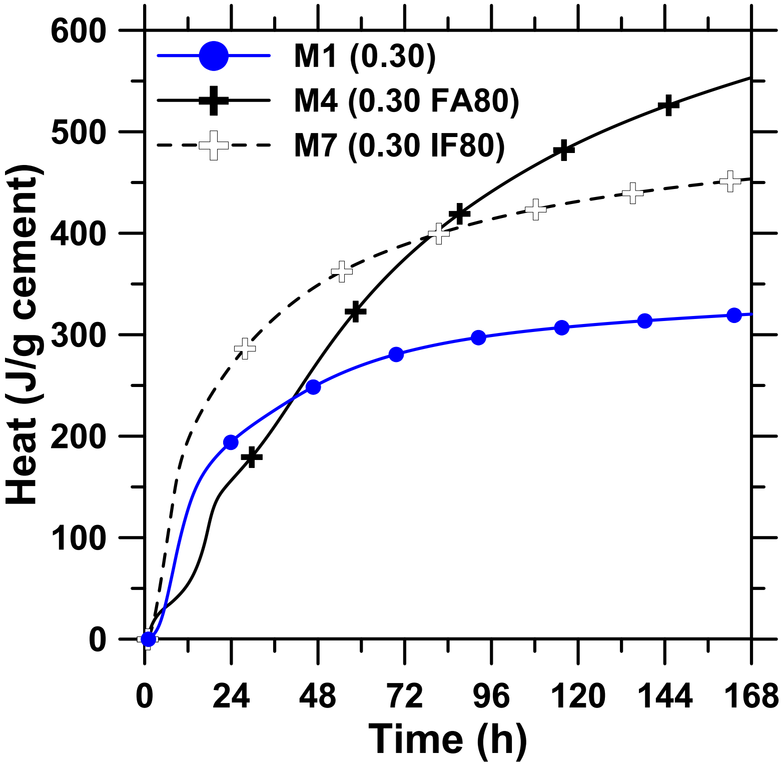

Figure 10. Heat release as a function of time. Comparison between *w/c* = 0.30 plain, and *w/cm* = 0.30 + 80 % fly ash or inert filler.

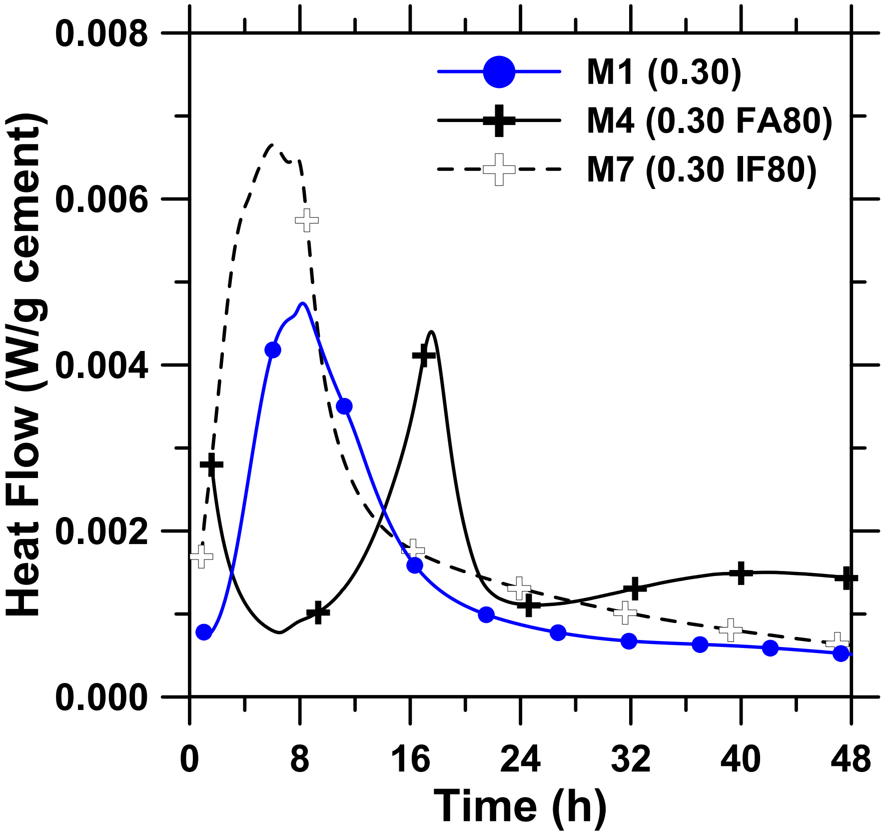

Figure 11. Heat flow as a function of time. Comparison between *w/c* = 0.30 plain, and *w/cm* = 0.30 + 80 % fly ash or inert filler.

High fly ash volume replacement levels (e.g., 60 % to 80 %) increase the sulfate demand. This can be observed in both Figures 9 and 11, where the spatial relationship between the gypsum depletion peak (typically the 2nd peak) and the main silicate peak is modified relative to the systems without fly ash [56]. As such, the hydration reaction of these systems might not be optimum, and the heat release and heat flow might be influenced by sulfate depletion. The effect of adding more sulfates to the mixture with 60 % fly ash replacement (M3) on the heat release and heat flow can be observed in Figures 12 and 13, respectively. Sulfates were added as 50 % calcium sulfate dehydrate (i.e., gypsum) and 50 % basanite (i.e., calcium sulfate hemihydrate or plaster), as described by Niemuth [56]. While a larger amount of heat release is observed (Figure 12), the main silicates hydration peak occurs at the same time as in the mixture with a lower sulfate content, thus not affecting its rate of reaction (Figure 13). As can be seen in the Figures, this particular fly ash causes an increasing retardation of the early-age hydration reactions as its volumetric replacement level is increased and this retardation is not corrected by a further addition of sulfate [21].

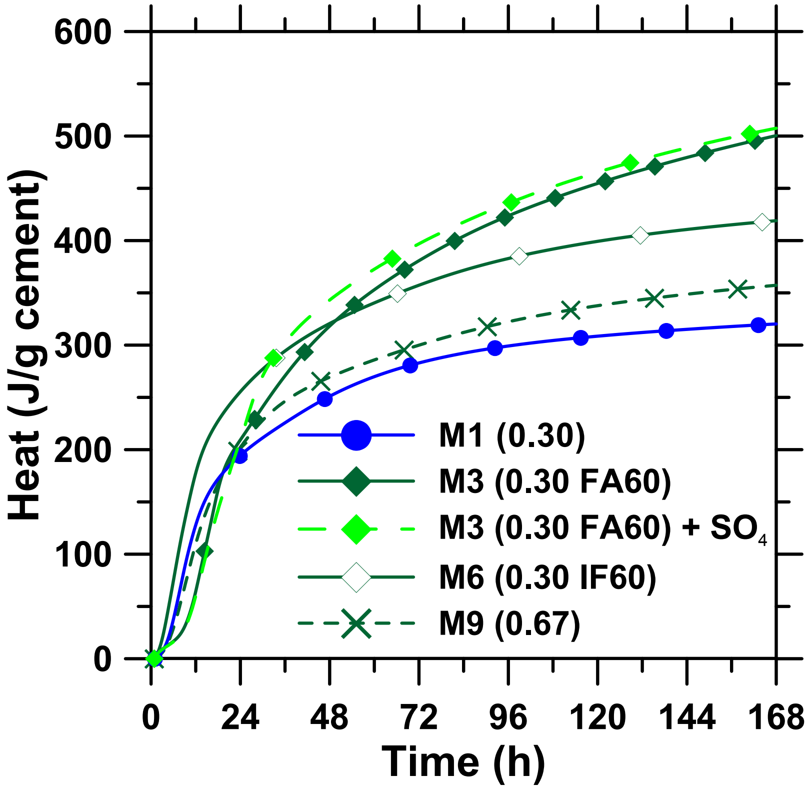

Figure 12. Effect of sulfate addition on the heat release of a 60 % fly ash mortar mixture.

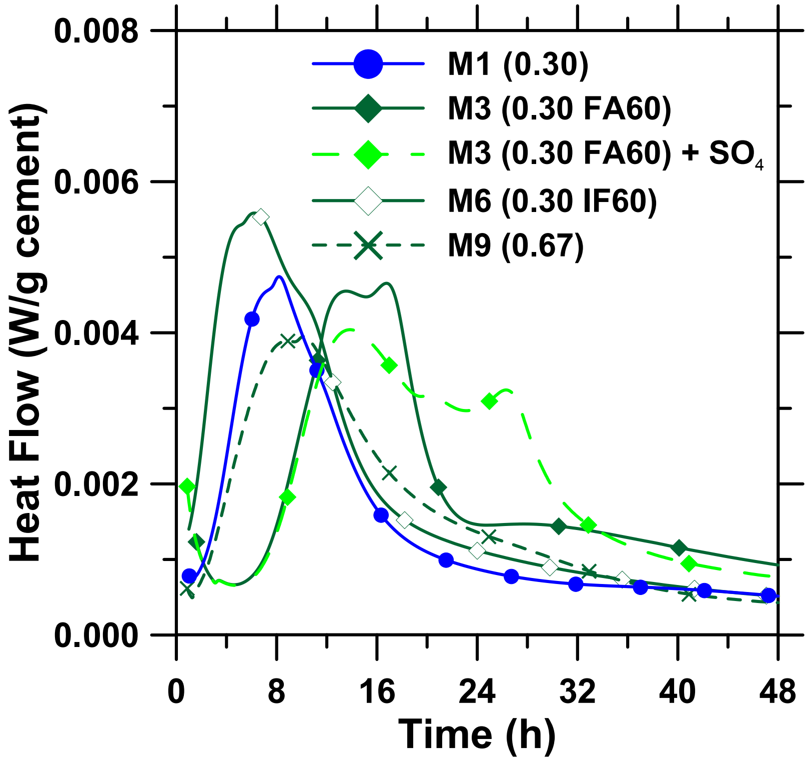

Figure 13. Effect of sulfate addition on the heat flow of a 60 % fly ash mortar mixture.

6.2. Internal Relative Humidity

Figure 14 shows the measured internal RH as a function of fly ash or inert filler replacement level. The RH decreases over time, due to self-desiccation or ‘internal drying’ caused by the hydration (and pozzolanic) reactions and their accompanying chemical shrinkage [11,50]. At 1 d, the RH is similar at all replacement levels between the fly ash and inert filler mixtures. However, at later ages, the RH of the fly ash mixtures is always lower than that of the inert filler mixtures. As time passes, the difference in magnitude of RH between the fly ash and the inert filler mixtures becomes larger. This is due to the chemical reactions of the fly ash that consume part of the water with accompanying chemical shrinkage, reducing the total RH of the system. The further reduction of RH in the fly ash mixtures compared to the inert filler mixtures is also an indication of the pore structure that is being formed. Lower RH implies smaller filled pore sizes, according to the Kelvin-Laplace equation [57], so it is expected to see a finer microstructure in the fly ash mixtures compared to the inert filler mixtures. Additionally, the difference in magnitude of RH between the fly ash and the inert filler mixtures at later ages is larger at higher replacement levels. These results imply that fly ash has a more dominant chemical effect at later ages, rather than a physical one.

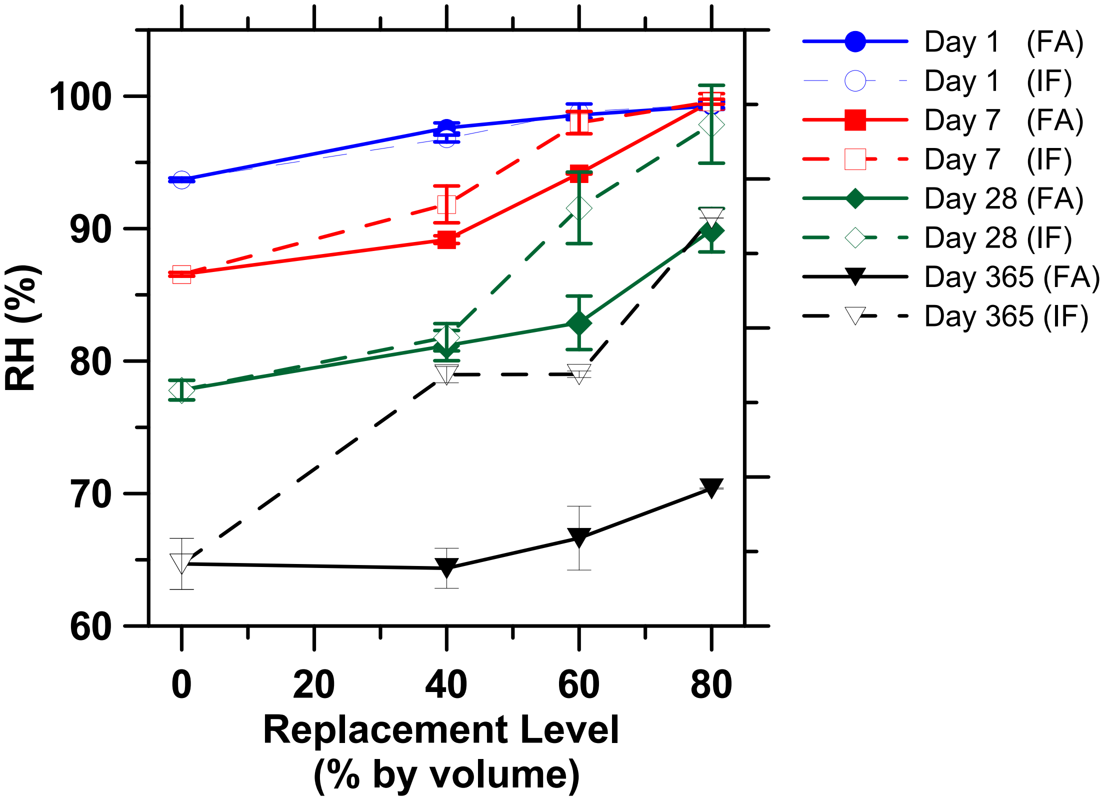

Figure 14. Effect of the addition of fly ash or inert filler on the internal relative humidity (Error bars represent ± one standard deviation of three specimens).

6.3. Electrical Impedance Spectroscopy

Isothermal calorimetry is a powerful tool used to evaluate the hydration reaction of cementitious materials at early ages. The results presented in previous sections allowed isolating the physical and chemical effects provided by the addition of fly ash during the first 7 d. However, isothermal calorimeters are not normally used for longer than 14 d, as the heat release signal-noise ratio becomes very small.

In mixtures containing high volumes of fly ash, the use of an isothermal calorimeter can sometimes be a limitation, since the fly ash reaction is typically slower than that of cement; thereby, most of the fly ash reaction may occur after the first 14 d. As such, other means need to be considered to indirectly evaluate the extent of reaction at later ages. One technique is by measuring the electrical properties of the material, via electrical impedance spectroscopy. This has been used in this study to evaluate the physical and chemical effects provided by the addition of fly ash at later ages (e.g., 3 months and 6 months).

The measured electrical conductivity in concrete samples will depend on three primary factors (if the temperature is held constant): 1) the liquid-filled pore volume, 2) the connectivity of the liquid-filled porosity, and 3) the electrical conductivity of the pore solution [58], as indicated in equation 2.

$$\sigma_t = \sigma_0 \cdot \emptyset \cdot \beta \qquad (2)$$

where σ_t is the measured total conductivity (S/m), σ_0 is the measured pore solution conductivity (S/m), $\emptyset$ is the capillary porosity, and β is the calculated pore connectivity factor.

It is commonly accepted that the main conductive phase is the liquid, as the resistance of this phase is many orders of magnitude less than any other phases [58]. When samples are kept sealed, the amount of liquid decreases, as it is consumed by the hydration reaction. However, smaller amounts of pore solution will not necessary yield a lower measured total conductivity, as the pore solution will concurrently become more concentrated in ions being dissolved from the cement particles, and therefore more electrically conductive. As such, measuring conductivity without knowing the conductivity of the pore solution and the volume of pores filled with solution may result in a misinterpretation of the results. Extraction of pore solution can be performed, but only with laborious methods at relatively early ages [59]. Moreover, at later ages (e.g., after 7 d), it may be impractical to obtain pore solution samples [60].

Figure 15 shows the results of electrical conductivity tests performed on the samples prepared with different amounts of fly ash or inert filler. As the fly ash volume replacement level increases, the electrical conductivity decreases. As observed in the calorimetry results (Figures 5, 8, 10), larger changes are achieved with larger amounts of fly ash, which implies more reaction. In other words, more hydration products are filling the pores, causing the disconnection of these pores, and therefore a lower measured electrical conductivity (increased formation factor). However, this trend is not observed in the specimen with 80 % of the cement being replaced with fly ash. This is probably due to a lack of calcium hydroxide at later ages (coming from the cement reaction) needed to react with the aluminates and silicates of the fly ash.

Likewise, it can be observed that as the inert filler replacement level increases, the electrical conductivity increases. This shows that at later ages, the physical effects (spacing and nucleation) are less predominant than the chemical effect (fly ash reactivity), as observed in Figure 7, where the slope of the fly ash reactivity curve is larger than that of the spacing and nucleation curves. If this is the case, the electrical conductivity of the fly ash mixtures at later ages is mainly controlled by the fly ash reaction. This does not occur in the inert filler mixtures, since the amount of reactive material (cement in that case) is lower. Then, more inert filler implies less reaction in the system (the inert filler is both a non-conductive and a non-reactive material). This is translated into less hydration products filling the pores (higher porosity), and consequently, higher conductivity values.

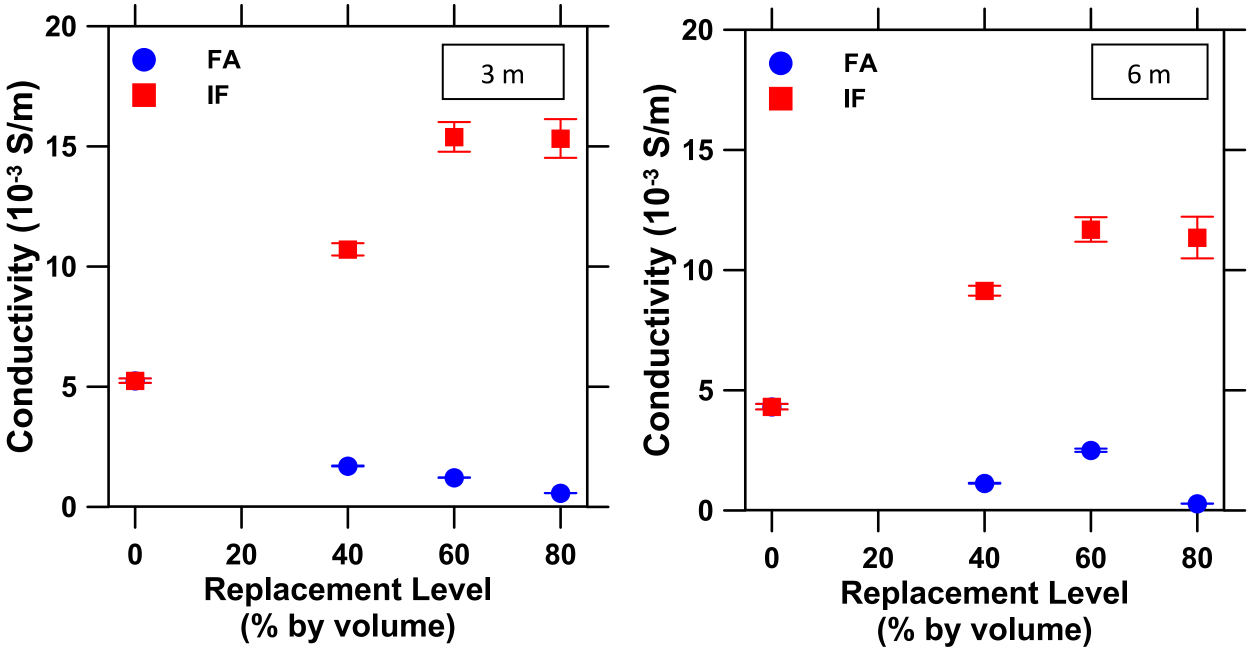

(a) (b)

Figure 15. Paste electrical conductivity as a function of replacement level at ages of (a) 3 months and (b) 6 months. (Error bars represent ± one standard deviation of three specimens).

As with the internal RH measurements, the electrical conductivity results show that the reaction of fly ash has a greater effect at later ages, since when comparing the inert filler mixtures with the fly ash mixtures, the measured conductivity is lower in the latter ones. The fly ash systems provide the same spacing factor and additional nucleation sites as the inert filler mixtures, as claimed throughout this study, therefore the difference in conductivity implies that the fly ash reaction controls the performance of these systems at later ages.

7. CONCLUSIONS

When fly ash is used in concrete it is generally believed that the fly ash will react (hydraulically or pozzolanically), providing increased reaction products, reduced porosity, and increased durability. In addition, fly ash can act as a filler, especially at very early ages, when it has not yet reacted chemically. The filler effect results in three factors that should be considered: 1) dilution (i.e., larger separation among cement particles), which promotes more complete cement hydration since more space is available, 2) increased dilution of the pore solution, and 3) provision of new nucleation sites that can promote the formation of more hydration products.

This paper has attempted to infer, from bulk, indirect measurements, the physical and chemical effects that high volumes of fly ash have on the cement hydration at both early and later ages. This was done using measurements from isothermal calorimetry, internal relative humidity, and electrical conductivity of high volume fly ash and chemically inert filler mortar mixtures. Three cement volume replacement levels have been used for this purpose: 40 %, 60 %, and 80 %. The cement was replaced with either fly ash or an inert filler (silica sand) with a similar gradation as that of the fly ash. By using the inert filler, the effects of increased cement particle spacing and additional nucleation sites were isolated from the chemical effect of fly ash reactivity.

The results indicate that the increased spacing of cement and nucleation effects provided by the addition of fly ash are dominant when compared with the chemical effect (i.e., fly ash reactivity) at early ages (less than 48 h), for the mixtures with a 40 % volume replacement level. This effect is even greater in mixtures with higher fly ash replacement levels. At early ages, the addition of the fly ash chosen for this study caused retardation in the system, as observed in the measured heat flow. The retardation is larger as the fly ash replacement level increases. After 48 h, the mixtures containing fly ash exhibited a greater cumulative heat release, which indicates a greater extent of hydration/reaction.

At later ages (3 months and 6 months), the internal relative humidity and electrical conductivity results indicate that the fly ash reactivity is more dominant than the spacing and nucleation effects, when comparing the electrical conductivity of samples with fly ash and inert filler. The fly ash mixtures have a lower RH compared to that of the inert filler mixtures which indicates greater reaction and a finer pore structure in the fly ash system.

The approach shown in this study decouples the physical and chemical effects of fly ash.

8. ACKNOWLEDGEMENTS

The research which is the subject of this document was funded by the U.S. Federal Highway Administration under contract DTFH61-08-R-00034. This support is gratefully acknowledged. The publication of this report does not necessarily indicate approval or endorsement of the findings, opinions, conclusions, or recommendations either inferred or specifically expressed herein by SES Group and Associates, the National Institute of Standards and Technology, Oregon State University, or Universidad del Desarrollo.

9. REFERENCES

[1] R.E. Davis, R.W. Carlson, J.W. Kelly, A.G. Davis, Properties of cements and concretes containing fly ash, in: Am. Concr. Inst., 1937: pp. 577–612. doi:10.14359/8435.

[2] W.J. Halstead, Use of fly ash in concrete, NCHRP Synth. Highw. Pract. (1986).

[3] R. Helmuth, Fly ash in cement and concrete, Portl. Cem. Assoc. (1987).

[4] V. Malhotra, A.A. Ramezanianpour, Fly ash in concrete, in: Energy, Mines Resour., CANMET, Ottawa, Canada, 1994: p. 307.

[5] ACI-232, Use of fly ash in concrete, ACI 232.2R ACI Comm. Rep. (1996) 34.

[6] V.M. Malhotra, Role of supplementary cementing materials in reducing greenhouse gas emissions, in: O. Gjorv, K. Sakai (Eds.), Concr. Technol. a Sustain. Dev. 21st Century, CANMET, 1999: p. 400.

[7] V.M. Malhotra, Making concrete "Greener" with fly ash, Concr. Int. 21 (1999) 61–66.

[8] E. Worrell, L. Price, N. Martin, C. Hendriks, L.O. Meida, Carbon Dioxide Emissions from the Global Cement Industry, Annu. Rev. Energy Environ. 26 (2001) 303–329. doi:10.1146/annurev.energy.26.1.303.

[9] P.K. Mehta, Greening of the concrete industry for sustainable development, Concr. Int. 24 (2002) 23–28.

[10] V.S. A. Bilodeau K. E. Painter, and V. M. Malhotra, Durability of Concrete Incorporating High Volumes of Fly Ash From Sources in the U.S.A., Mater. J. 91 (n.d.). doi:10.14359/4411.

[11] I. De la Varga, J. Castro, D.P. Bentz, J. Weiss, Application of internal curing for mixtures containing high volumes of fly ash, Cem. Concr. Compos. 34 (2012) 1001–1008. doi:10.1016/j.cemconcomp.2012.06.008.

[12] I. De la Varga, R.P. Spragg, C. Di Bella, J. Castro, D.P. Bentz, J. Weiss, Fluid transport in high volume fly ash mixtures with and without internal curing, Cem. Concr. Compos. 45 (2014) 102–110. doi:10.1016/j.cemconcomp.2013.09.017.

[13] E.E. Berry, V.M. Malhotra, Fly ash for use in concrete - A critical review, ACI J. Proc. 77 (1980) 59–73. doi:10.14359/6991.

[14] E. Sakai, S. Miyahara, S. Ohsawa, S.-H. Lee, M. Daimon, Hydration of fly ash cement, Cem. Concr. Res. 35 (2005) 1135–1140. doi:10.1016/j.cemconres.2004.09.008.

[15] S. Ng, H. Justnes, Influence of plasticizers on the rheology and early heat of hydration of blended cements with high content of fly ash, Cem. Concr. Compos. 65 (2016) 41–54. doi:10.1016/j.cemconcomp.2015.10.005.

[16] D.P. Bentz, C.F. Ferraris, I. De la Varga, M.A. Peltz, J.A. Winpigler, Mixture

proportioning options for improving high volume fly ash concretes, Int. J. Pavement Res. Technol. 3 (2010) 234–240.

[17] A.L.A. Fraay, J.M. Bijen, Y.M. De Haan, The reaction of fly ash in concrete a critical examination, Cem. Concr. Res. 19 (1989) 235–246. doi:10.1016/0008-8846(89)90088-4.

[18] K. Wesche, Fly ash in concrete: properties and performance, in: CRC Press LLC, 1991.

[19] P.C. Aitcin, W. Wilson, S. Mindness, Increasing the strength of concretes made with blended cements: Physical approach to increasing packing density of binder particles, Concr. Int. 38 (2016) 49–52.

[20] K. Hong, H. Justnes, M. Geiker, Early age strength increase of fly ash blended cement by a ternary hardening accelerating admixture, Cem. Concr. Res. 81 (2016) 59–69. doi:10.1016/j.cemconres.2015.11.004.

[21] D.P. Bentz, C.F. Ferraris, K.A. Snyder, Best practices guide for high-volume fly ash concretes: assuring properties and performance, NIST Tech. Note 1812, U.S. Dep. Commer. (2013).

[22] K. De Weerdt, M. Ben Haha, G. Le Saout, K.O. Kjellsen, H. Justnes, B. Lothenbach, Hydration mechanisms of ternary Portland cements containing limestone powder and fly ash, Cem. Concr. Res. 41 (2011) 279–291. doi:10.1016/j.cemconres.2010.11.014.

[23] D.P. Bentz, Activation energies of high-volume fly ash ternary blends: Hydration and setting, Cem. Concr. Compos. 53 (2014) 214–223. doi:10.1016/j.cemconcomp.2014.06.018.

[24] C.-W. Chung, P. Suraneni, J.S. Popovics, L.J. Struble, Setting time measurement using ultrasonic wave reflection, ACI Mater. J. 109 (2012) 109. http://usherbrooke.summon.serialssolutions.com/2.0.0/link/0/eLvHCXMwXZ27CgIxEEWD-AWCr84fiCSZ7Ey2XnYRbN3CSvKYVIv4_5WzPkAs5g8ul3uKwygF7mj0XyeYiFQIs52VrmAhcpZgYMixJK7VvF3l8dp057b_KfhhpRZ8X6tx6C_dSX_-A-iHrASnfeszFZnEiCyck3zFagMFFGZp2AecRZZKsyvsCX2saBNgEYRwiTJ.

[25] X. Feng, E.J. Garboczi, D.P. Bentz, P.E. Stutzman, T.O. Mason, Estimation of the degree of hydration of blended cement pastes by a scanning electron microscope point-counting procedure, Cem. Concr. Res. 34 (2004) 1787–1793. doi:10.1016/j.cemconres.2004.01.014.

[26] R. Snellings, K.L. Scrivener, Rapid screening tests for supplementary cementitious materials: past and future, Mater. Struct. 49 (2016) 3265–3279. doi:10.1617/s11527-015-0718-z.

[27] P.T. Durdziński, C.F. Dunant, M. Ben Haha, K.L. Scrivener, A new quantification method based on SEM-EDS to assess fly ash composition and study the reaction of its individual components in hydrating cement paste, Cem. Concr. Res. 73 (2015) 111–122. doi:10.1016/j.cemconres.2015.02.008.

[28] S.A. Bernal, M.C.G. Juenger, X. Ke, W. Matthes, B. Lothenbach, N. De Belie, J.L. Provis, Characterization of supplementary cementitious materials by thermal analysis, Mater. Struct. 50 (2016) 1–13. doi:10.1617/s11527-016-0909-2.

[29] S. Bae, C. Meral, J. Oh, J. Moon, M. Kunz, P.J.M. Monteiro, Characterization of morphology and hydration products of high-volume fly ash paste by monochromatic scanning x-ray micro-diffraction (μ-SXRD), Cem. Concr. Res. 59 (2014) 155–164. doi:10.1016/j.cemconres.2014.03.001.

[30] M. Aboustait, T. Kim, M.T. Ley, J.M. Davis, Physical and chemical characteristics of fly

ash using automated scanning electron microscopy, Constr. Build. Mater. 106 (2016) 1–10. doi:10.1016/j.conbuildmat.2015.12.098.

[31] K.L. Aughenbaugh, R.T. Chancey, P. Stutzman, M.C. Juenger, D.W. Fowler, An examination of the reactivity of fly ash in cementitious pore solutions, Mater. Struct. 46 (2013) 869–880. doi:10.1617/s11527-012-9939-6.

[32] R.T. Chancey, P. Stutzman, M.C.G. Juenger, D.W. Fowler, Comprehensive phase characterization of crystalline and amorphous phases of a Class F fly ash, Cem. Concr. Res. 40 (2010) 146–156. doi:10.1016/j.cemconres.2009.08.029.

[33] B. Lothenbach, K. Scrivener, R.D. Hooton, Supplementary cementitious materials, Cem. Concr. Res. 41 (2011) 1244–1256. doi:10.1016/j.cemconres.2010.12.001.

[34] V.M. Malhotra, Durability of concrete incorporating high-volume of low-calcium (ASTM Class F) fly ash, Cem. Concr. Compos. 12 (1990) 271–277. doi:10.1016/0958-9465(90)90006-J.

[35] J.W. Bullard, H.M. Jennings, R.A. Livingston, A. Nonat, G.W. Scherer, J.S. Schweitzer, K.L. Scrivener, J.J. Thomas, Mechanisms of cement hydration, Cem. Concr. Res. 41 (2011) 1208–1223. doi:10.1016/j.cemconres.2010.09.011.

[36] P. Termkhajornkit, T. Nawa, K. Kurumisawa, Effect of water curing conditions on the hydration degree and compressive strengths of fly ash–cement paste, Cem. Concr. Compos. 28 (2006) 781–789. doi:10.1016/j.cemconcomp.2006.05.018.

[37] N. Chousidis, I. Ioannou, E. Rakanta, C. Koutsodontis, G. Batis, Effect of fly ash chemical composition on the reinforcement corrosion, thermal diffusion and strength of blended cement concretes, Constr. Build. Mater. 126 (2016) 86–97. doi:10.1016/j.conbuildmat.2016.09.024.

[38] G.D. Moon, S. Oh, Y.C. Choi, Effects of the physicochemical properties of fly ash on the compressive strength of high-volume fly ash mortar, Constr. Build. Mater. 124 (2016) 1072–1080. doi:10.1016/j.conbuildmat.2016.08.148.

[39] F. Zunino, M. Lopez, Decoupling the physical and chemical effects of supplementary cementitious materials on strength and permeability: A multi-level approach, Cem. Concr. Compos. 65 (2016) 19–28. doi:10.1016/j.cemconcomp.2015.10.003.

[40] D.P. Bentz, E.J. Garboczi, K.A. Snyder, A hard core/soft shell microstructural model for studying percolation and transport in three-dimensional composite media, NISTIR 6265, U.S. Dep. Commer. (1999).

[41] D.P. Bentz, C.F. Ferraris, S.Z. Jones, D. Lootens, F. Zunino, Limestone and Silica Powder Replacements for Cement: Early-Age Performance, Cem. Concr. Compos. (2016).

[42] M. Cyr, P. Lawrence, E. Ringot, Mineral admixtures in mortars: Quantification of the physical effects of inert materials on short-term hydration, Cem. Concr. Res. 35 (2005) 719–730. doi:10.1016/j.cemconres.2004.05.030.

[43] T. Oey, A. Kumar, J.W. Bullard, N. Neithalath, G. Sant, The Filler Effect: The Influence of Filler Content and Surface Area on Cementitious Reaction Rates, J. Am. Ceram. Soc. 96 (2013) 1978–1990. doi:10.1111/jace.12264.

[44] Mixture Proportioning for Internal Curing with Lightweight Aggregates, (2010). http://ciks.cbt.nist.gov/~bentz/intcuring.html.

[45] E.J. Garboczi, J.W. Bullard, Shape analysis of a reference cement, 2004. doi:10.1016/j.cemconres.2004.01.006.

[46] ASTM C305-14, Standard practice for mechanical mixing of hydraulic cement pastes and mortars of plastic consistency, ASTM International, West Conshohocken, PA, 2014.

doi:10.1520/C0305-14.
[47] D.P. Bentz, C.F. Ferraris, Rheology and setting of high volume fly ash mixtures, Cem. Concr. Compos. 32 (2010) 265–270. doi:10.1016/j.cemconcomp.2010.01.008.
[48] H. Le Chatelier, Sur les changements de volume qui accompagnent le durcissement des ciments, 5th ed., Bulletin Société de l'Encouragement pour l'Industrie Nationale, Paris, France, 1900.
[49] R.G. L'Hermite, Volume changes of concrete, in: 4th Int. Symp. Chem. Cem., Washington DC, 1960.
[50] O.M. Jensen, P.F. Hansen, Water-entrained cement-based materials: I. Principles and theoretical background, Cem. Concr. Res. 31 (2001) 647–654. doi:10.1016/S0008-8846(01)00463-X.
[51] L. Greenspan, Humidity fixed points of binary saturated aqueous solutions, J. Res. Natl. Bur. Stand. Sect. A Phys. Chem. 81A (1977) 89. doi:10.6028/jres.081A.011.
[52] J. Castro, R. Spragg, J. Weiss, Water absorption and electrical cnductivity for internally cured mortars with a W/C between 0.30 and 0.45, J. Mater. Civ. Eng. 24 (2012) 223–231. doi:10.1061/(ASCE)MT.1943-5533.0000377.
[53] ASTM C1702-15, Standard Test Method for Measurement of Heat of Hydration of Hydraulic Cementitious Materials Using Isothermal Conduction Calorimetry, ASTM International, West Conshohocken, PA, 2015.
[54] J. Castro, I. De la Varga, J. Weiss, Using isothermal calorimetry to assess the water absorbed by fine LWA during mixing, J. Mater. Civ. Eng. 24 (2012) 996–1005. doi:10.1061/(ASCE)MT.1943-5533.0000496.
[55] D.P. Bentz, M.A. Peltz, J. Winpigler, Early-age properties of cement-based materials. II: Influence of water-to-cement ratio, J. Mater. Civ. Eng. 21 (2009) 512–517. doi:10.1061/(ASCE)0899-1561(2009)21:9(512).
[56] M.D. Niemuth, Effect of fly ash on the optimum sulfate of Portland Cement., Purdue University, 2012.
[57] J. Castro, D. Bentz, J. Weiss, Effect of sample conditioning on the water absorption of concrete, Cem. Concr. Compos. 33 (2011) 805–813. doi:10.1016/j.cemconcomp.2011.05.007.
[58] F. Rajabipour, Insitu electrical sensing and material health monitoring in concrete structures, Purdue University, 2006.
[59] M. Penko, Some early hydration processes in cement paste as monitored by liquid phase composition measurements, Purdue University, 1983.
[60] R.S. Barneyback, S. Diamond, Expression and analysis of pore fluids from hardened cement pastes and mortars, Cem. Concr. Res. 11 (1981) 279–285. doi:10.1016/0008-8846(81)90069-7.